SPARSE BEAMFORMING FOR ACTIVE UNDERWATER ELECTROLOCATION

Nam Nguyen, Ingo Wiegand and Douglas L. Jones

Coordinated Science Laboratory
University of Illinois at Urbana Champaign

ABSTRACT

Weakly electric fish have the ability to navigate and locate prey in the dark using a unique weak electrosense system. Imitating that ability of electric fish, we develop an electric-field sensing system capable of high-resolution imaging of the surrounding environment, by use of a novel beamforming technique that exploits the sparsity of sources in a scanned space. Both simulation and experimental results show that the sparse beamforming technique accurately images not only a single object but also multiple objects with highly correlated signals.

Index Terms— Weakly electric fish, electrosensors, electrolocation, sparse beamforming, basis pursuit.

1. INTRODUCTION

Weakly electric fish have been a subject of intense study in neurobiology for their ability to emit and sense electric fields. This ability allows them to hunt in total darkness and muddy environments where vision becomes useless [1, 2]. While biologists aim at understanding this sensory mechanism in fish [3, 4], engineers, on the other hand, focus on applying the understanding to design systems and techniques that can imitate this ability. Recent works by MacIver et al show that they can build robotic systems with an electric sense to locate and track objects either underwater or in the air [5, 6, 7].

Our work advances one step further by devising an electric-field sensing system that is able not only to localize an object but also to image the surrounding environment, even with multiple objects. Such a 'distant touch' imaging sense would be an invaluable attribute for future underwater vehicles in intrusion detection, target tracking and especially, close-in maneuvering. In fact, our previous work [8, 9] also developed a near-field sensing system using biomimetic fluid-flow sensors to image local fluid-flow sources in water. In that work, we used a Capon (MVDR) adaptive beamforming technique to generate near-field images. However, the Capon method and other conventional beamforming techniques fail for multiple objects when they are highly correlated.

This work was supported by the DARPA BioSenSE Program under Grant FA-9550-05-1-0459.

In this paper, we develop a novel sparse beamforming technique that assumes that the image of multiple sources in the surrounding environment is actually sparse. The beamforming problem can then be transformed into a sparse signal reconstruction problem $\mathbf{A}\mathbf{x} = \mathbf{b}$, where each entry of the vector $\mathbf{x}$ represents the presence of an object at a given location, each column vector of the matrix $\mathbf{A}$ represents the expected sensor outputs for the location corresponding to the same row in $\mathbf{x}$, and $\mathbf{b}$ is the sensor measurements. Since there are typically relatively few sources present in the scanned space, the vector $\mathbf{x}$ has a small number of non-zero entries. Our problem then becomes the well-known problem of solving an under-determined linear system of equations under a sparsity condition [10]. Many algorithms have been proposed to solve this problem, and we use a *Basis Pursuit* method which turns this problem into an ℓ_1-minimization problem which can be solved by linear programming [11].

2. UNDERWATER ELECTROLOCATION MODEL

Placing an object with a different conductivity than the surroundings in an electric field alters the field. If the object is conductive, the electric field moves the free electrons to one side of the object and creates an induced electric dipole. In general, when a relatively small sphere of radius a with conductivity σ_{object} is placed in water with conductivity σ_{water} at the point $\vec{\mathbf{r}}$ with electric field $\vec{\mathbf{E}}_f$, the perturbation caused by the induced electric field was derived in [3]:

$$\Delta\phi(\vec{\mathbf{r}}) = \frac{a^3 \mathbf{E}_f . \vec{\mathbf{r}}}{\|\vec{\mathbf{r}}\|^3} \left(\frac{\sigma_{\text{object}} - \sigma_{\text{water}}}{\sigma_{\text{object}} + 2\sigma_{\text{water}}} \right), \tag{1}$$

where $\Delta\phi(\vec{\mathbf{r}})$ is the change in potential at position $\vec{\mathbf{r}}$ relative to the sphere's center and $\|.\|$ is the magnitude of a vector. Based on the model in (1), we design an electric-field sensing system consisting of two electrodes to form an electric dipole and an array of electric-field sensors aligned with the electrodes as shown in Figure 1. This is crudely analogous to the biological system found in a weakly electric fish, which generates an oscillating electric field at its head and tail and which has several hundred electrosensors distributed across its body. In our system, the electric-field sensors are simply made of pairs of electrodes placed symmetrically about the

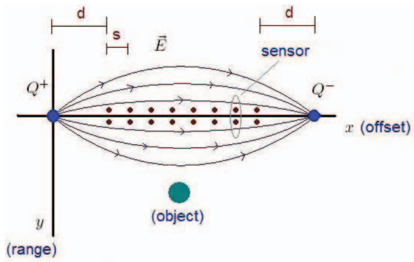

Fig. 1. A weakly electric field sensing system

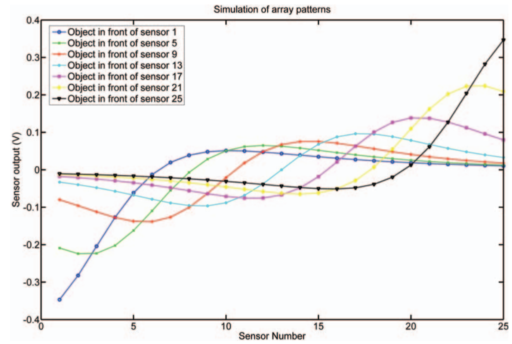

Fig. 2. Array patterns in simulation of a weakly electrical sensing system as shown in Figure 1 with 25 sensors, $d = 50$ mm, $s = 8$ mm. For each pattern, the object stays 70 mm away from the array and in front of one specified sensor.

dipole axis. If the dipole has charges of $+Q$ and $-Q$, then the electrostatic field at a point is

$$\vec{\mathbf{E}}_f = \frac{Q}{4\pi\epsilon}\left(\frac{\vec{\mathbf{r}}_{Q^+}}{\left\|\vec{\mathbf{r}}_{Q^+}\right\|^3} - \frac{\vec{\mathbf{r}}_{Q^-}}{\left\|\vec{\mathbf{r}}_{Q^-}\right\|^3}\right), \tag{2}$$

where $\vec{\mathbf{r}}_{Q^+}$ and $\vec{\mathbf{r}}_{Q^-}$ are vectors originating from the point of interest to the electrodes Q^+ and Q^-, respectively. Without an object in the field, each sensor should see zero voltage across its pair of electrodes. When an object is placed in the field, the perturbation caused by the object can be measured in term of voltages across all sensors based on equations (1) and (2). These perturbations on the sensors form an array pattern. The array pattern changes according to the position of the object. Figure 2 shows the simulated array patterns for different object positions; an object at different locations produces distinct array patterns. The array patterns, or more precisely the relative shape of the patterns, can be used to estimate the locations of the object without the knowledge of its size and conductivity.

The localization problem can be approached using a generalized beamforming technique, which means scanning all possible positions and identifying ones that maximize a likelihood function. In recent work [8], we used Capon's beamforming technique for a similar problem of mapping the location of a vibrating object in water sensed by an array of underwater fluid-flow sensors. However, locating multiple objects with this method requires that their signals be uncorrelated, which is not possible when all signals are induced by a common active source. In this work, we propose a new beamforming technique that turns the localization problem into solving an underdetermined linear system of equations $\mathbf{Ax} = \mathbf{b}$ with sparse solutions.

3. SPARSE BEAMFORMING

In this section, we show that the localization problem above can be solved as an underdetermined linear system of equations with sparse solutions. Consider a discrete 2D localization problem in which we sample the plane on a 2D grid with N points. For each position of the object on the grid, we compute the expected array pattern (i.e., the vector of voltage differences across the array of sensor pairs) using the model in Equation (1). For the n-th point in the grid, we denote the expected array pattern as $\mathbf{a}(n) = [a_1(n), a_2(n), \ldots, a_K(n)]^T$, where K is the number of sensors in the array. Scanning all N points on the grid, we form an $L \times N$ matrix

$$\mathbf{A} = [\mathbf{a}(1), \mathbf{a}(2), \ldots, \mathbf{a}(N)].$$

An object located at an unknown point on the grid induces a pattern $\mathbf{b} = [b_1, b_2, \ldots, b_K]^T$. The vector $\mathbf{b}$ must be equivalent to some column i in the matrix $\mathbf{A}$. With multiple small objects that do not significantly distort the overall field, this problem reduces to solving $\mathbf{Ax} = \mathbf{b}$, where $\mathbf{x}$ is a length-N vector with all zero elements except the elements corresponding to the object locations. In most cases, $N >> K$ and the equation $\mathbf{Ax} = \mathbf{b}$ is a highly underdetermined linear system of equations. This system has infinitely many solutions but under the condition to maximize sparsity of the solution, a unique solution can be found. Many algorithms have been proposed to solve this problem [10]. In this paper, we cast our problem as an ℓ_1-minimization problem

$$\min \|\mathbf{x}\|_1, \quad \text{subject to} \quad \mathbf{Ax} = \mathbf{b},$$

which can be effectively solved via a linear program [11]. In the next two sections, we demonstrate the performance of this beamforming method in simulations and especially in experiments where a vector $\mathbf{b}$ of real data is imaged correctly with a matrix $\mathbf{A}$ derived from the idealized theoretical model.

4. SIMULATIONS

To test the idea of sparse beamforming for underwater electrolocation, we simulate a weakly electric sensing system as shown in Figure 1 with an array of $K = 25$ sensors. The distances between sensors are $s = 8$ (mm) and the distances from the dipole electrodes to the nearest sensors are $d = 50$ (mm). All other parameters (such as the dipole charges, the conductivity of water and of the object, and the radius of the

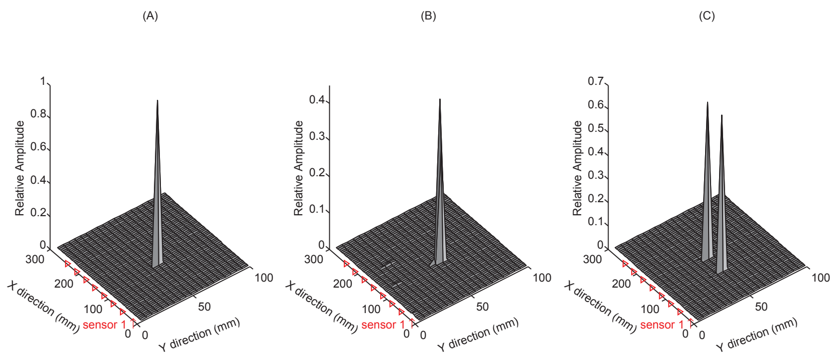

Fig. 3. *A)* Image of mapping an ideal simulated object at $x = 125$ mm and $y = 50$ mm. *B)* Image of mapping an noisy simulated object at x = 125 mm and y = 50 mm. *C)* Image of mapping two ideal simulated objects at x_1 = 100 mm, y_1 = 50 mm and x_2 = 150 mm, y_2 = 50 mm.

object in Equation (1)) can be combined as a constant gain factor. This factor will be cancelled out during normalization of array patterns $\mathbf{a}(n)$ so those parameters can take any values.

The first step is to form a 2-D grid of probing points then build the matrix $\mathbf{A}$ as a dictionary of all array patterns for each point on the grid. Note that each array pattern is normalized before forming a column in the matrix $\mathbf{A}$. Next, we select one array pattern $\mathbf{b}$ corresponding to a point of interest on the grid. This pattern is used as the measurement from the sensor array to estimate the position of the object. To solve the ℓ_1-minimization problem

$$\min \|\mathbf{x}\|_1, \quad \text{subject to} \quad \mathbf{Ax} = \mathbf{b},$$

we use the primal-dual interior-point method from the ℓ*1magic* package [12]. Figure 3 shows the results of imaging a single simulated object located at position $x = 125$ mm and $y = 50$ mm. We actually analyze two cases of sensor measurement with and without noise. For the case of no noise in the sensor output, Figure 3A displays a single sharp peak exactly at the original position of the object. In the presence of noise (SNR $\approx$ 20dB) in sensor outputs, Figure 3B shows a lower peak at the original position and a few small peaks close to the sensor array. Furthermore, we also test the capability of the beamforming technique to localize multiple sources. Figure 3C shows two separate peaks corresponding to exact locations of two simulated objects at x_1 = 100 mm, y_1 = 50 mm and x_2 = 150 mm, y_2 = 50 mm.

The simulation results demonstrate the potential of the sparse beamforming technique. In the next section, we demonstrate the effectiveness of this technique in an experimental setting.

5. EXPERIMENT AND RESULTS

5.1. Experiment Setup

A weakly electric sensing system was built according to the design in Figure 1. Using LEGO components, we set up a small rack to attach 7 pairs of electrodes serving as 7 sensors. Another pair of electrodes forms a dipole to generate an electric field. The legs of the 16 electrodes are placed in a basin of somewhat salty water as shown in Figure 4A. The distance between the sensors is $s = 32$ mm. The gap between the two electrodes of a sensor is 25.4 mm. The distance from the dipole electrodes to the nearest sensor is $d = 50$ mm. A square waveform of 1kHz with magnitude of 5 Volts drives the dipole to generate an electric field. Those configuration parameters are used to generate the dictionary matrix $\mathbf{A}$ from the theoretical model as in the simulation (Sec. 4). The only difference from the simulation is that we measure the real sensors' outputs when an object is brought near the sensor array.

5.2. Calibration

One challenge of working with a real sensor array is that we must first figure out the gain of each sensor to calibrate the array. For our sensor array, the calibration process is performed by moving a pair of test electrodes with a fixed spacing and voltage over each sensor. When the test electrodes move in front of a sensor, the output of that sensor is recorded and used to work out the gain of that sensor in the array.

In the model, we assume that the sensors' legs are symmetrical on both sides of the dipole's axis so that the voltages across each sensor are perfectly zero. It is not the case for the real experimental setting. In fact, we first carefully tune each sensor to get the lowest possible output voltage before putting an object in and recording the perturbations.

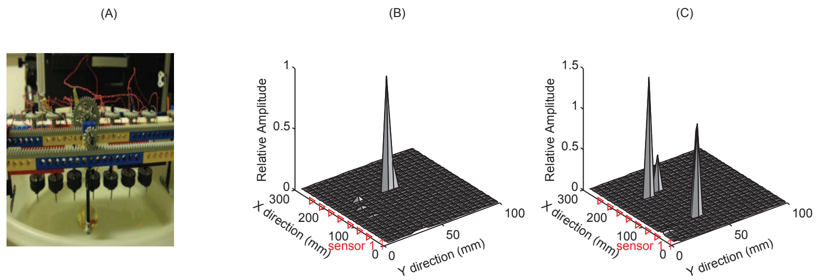

Fig. 4. *A)* Experimental setup. *B)* Image of successfully mapping a plastic ball at about 45 mm in front of Sensor 5. *C)* Image of mapping simultaneously two plastic ball objects at about 45 mm in range and between Sensors 1 & 2 and Sensors 5 & 6.

5.3. Single Object Mapping

In this experiment, we put a nonconductive plastic ball into the space in front of the sensor array. We recorded the sensor outputs for several positions in front of some sensors or in the gap between them. Figure 4B shows the results of mapping the location of the ball when it lies about 45 to 50 mm in front of Sensor 5. In those plots, we can clearly see one large peak very close to the expected location of the ball.

5.4. Multiple Objects Mapping

We then tested our sparse beamforming technique for multiple sources. Note that signals from multiple sources in the weakly electric sensing system are highly correlated as they are induced from the same dipole source, so conventional beamforming techniques do not work for this case. In the experiment, we put 2 similar plastic balls in 2 positions roughly between sensors 1 and 2 and between sensors 5 and 6. Both balls were at a range of about 45 to 50 mm away from the sensor array. The results displayed in Figure 4 clearly show that we can separate two sources and map the locations accurately.

6. CONCLUSION

Two contributions are made in this paper. We present the first weakly electric field sensing system with the ability of imaging surrounding objects in the near field. We also provide a new sparse beamforming technique that can overcome the challenge of separating correlated multiple sources. This has potential to spur future research into customizing the ℓ_1 minimization algorithm for beamforming applications.

7. REFERENCES

[1] T. H. Bullock and W. Heiligenberg, *Electroreception*, Wiley New York, 1986.

[2] R.W. Turner, L. Maler, and M. Burrows, *Electroreception and Electrocommunication*, Co. of Biologists Ltd., 1999.

[3] B. Rasnow, "The effects of simple objects on the electric field of Apteronotus," *Journal of Comparative Physiology A: Sensory, Neural, and Behavioral Physiology*, vol. 178, no. 3, pp. 397–411, 1996.

[4] B. Rasnow, "Measuring and visualizing EOD fields," *Communication in Fishes*, 2006.

[5] J.R. Solberg, K.M. Lynch, and M.A. MacIver, "Robotic Electrolocation: Active Underwater Target Localization with Electric Fields," *Proceedings of the 2007 International Conference on Robotics and Automation (ICRA) April*, pp. 10–14, 2007.

[6] M.A. MacIver and M.E. Nelson, "Towards a Biorobotic Electrosensory System," *Autonomous Robots*, vol. 11, no. 3, pp. 263–266, 2001.

[7] M.A. MacIver, E. Fontaine, and J.W. Burdick, "Designing future underwater vehicles: principles and mechanisms of the weakly electric fish," *Oceanic Engineering, IEEE Journal of*, vol. 29, no. 3, pp. 651–659, 2004.

[8] S. Pandya, Y. Yang, C. Liu, and D.L. Jones, "Biomimetic Imaging of Flow Phenomena," *Acoustics, Speech and Signal Processing, ICASSP 2007. IEEE International Conference on*, vol. 2, 2007.

[9] N. Nguyen, D.L. Jones, S. Pandya, Y. Yang, N. Chen, C. Tucker, and C. Liu, "Biomimetic Flow Imaging with an Artificial Fish Lateral Line," in *BIOSIGNALS (2)*, 2008, pp. 269–276.

[10] A. Bruckstein, D.L. Donoho, and M. Elad, "From sparse solutions of systems of equations to sparse modeling of signals and images," *SIAM ReviewTo appear*.

[11] S.S. Chen, D.L. Donoho, and M.A. Saunders, "Atomic Decomposition by Basis Pursuit," *SIAM JOURNAL ON SCIENTIFIC COMPUTING*, vol. 20, pp. 33–61, 1999.

[12] "http://www.acm.caltech.edu/l1magic/," .